

Stability-Constrained Microgrid Operation Scheduling Incorporating Frequency Control Reserve

Yiwei Wu, *Student Member, IEEE*, Gino J. Lim, *IEEE Member*, Jian Shi, *Member, IEEE*

Abstract—This paper presents a two-stage microgrid scheduling strategy in which the frequency control reserve (FCR) is incorporated to ensure economic, reliable and stable microgrid operation in a joint energy and ancillary service market environment. In addition to using such reserve to limit frequency excursions caused by uncertainties of active loads and renewable generation, this paper is focused on determining the optimal provision of reserve for microgrid operation mode switching to assure sufficient reserve is available and readily deployable at the disposal of the microgrid operator. The scheduling problem is formulated as a two-stage chance-constrained programming (CCP) model where the power balance chance constraints are used to determine the trade-off between operational economy and stability risk exposure. The chance-constrained formulation is then approximated as a deterministic mixed-integer linear programming (MILP) model for solution. Two sets of policy studies are performed through simulation to evaluate the effectiveness of the proposed strategy in enhancing the operational performance of a microgrid through optimal scheduling.

Index Terms—ancillary service, chance-constrained, frequency regulation, joint market, microgrid, optimal scheduling

NOMENCLATURE

Index

i	Dispatchable generation unit subscript index, $i \in D$
j	Non-dispatchable generation unit subscript index, $j \in M$
k	Load subscript index, $k \in L$
s	Scenario subscript index
t	Index for time periods

Parameters

c_i^g / c_i^r	Operation/reserve cost function for dispatchable generation unit i
$I_{s,t}^{grid}$	Grid-connect binary indicator for scenario s at time t , 1 for grid-connected mode
$I_{s,t}^{island}$	Islanding binary indicator for scenario s at time t , 1 for island mode
$l_{k,t,s}$	Microgrid load k at time t for scenario s
$q^{c,max/min}$	Max/min power output capacity of the utility grid at the point of common coupling
$q^{g,max/min}$	Max/min dispatchable unit power output capacity
$q_{j,t}^w$	Non-dispatchable generation unit j output
$R_i^{dw/up,max/min}$	Max/min i ramp up/down reserve capacity
RD_i / RU_i	Ramp-down/up cost of dispatchable generation unit i
SD_i / SU_i	Shut-down/startup cost of dispatchable generation unit i
T_i^{off} / T_i^{on}	Minimum off/on time of dispatchable generation unit i
$VOLL$	Value of load shedding

$VOPC$	Value of power curtailment
$X_{i,t}^{off/on}$	Off/on time of dispatchable generation unit i at time t
α_i / β_i	Penalty cost when microgrid is in grid-connected/island mode
$\rho_i^{c/r}$	Utility market power/ reserve price function
Sets	
D	Dispatchable generation unit set
L	Load set
M	Non-dispatchable generation unit set
Variables	
$b_{i,t}$	On/Off status of dispatchable unit i at time t
$l_{s,t}^{sh} / q_{s,t}^{cu}$	Load shedding/ power curtailment value at time t in scenario s
q_t^c	Power exchange at point of common coupling at time t
$q_{i,t}^g$	Dispatchable generation units output i at time t
$x_{i,t} / y_{i,t}$	Startup/Shutdown status of dispatchable unit i at time t
$r_{i,t,s}^{dw/up}$	Ramp-down/up reserve provided by dispatchable generation unit i at time t in scenario s in the second stage
$r_{t,s}^{dw/up,c}$	Ramp-down/up reserve provided by the utility grid at the point of common coupling at time t in scenario s in the second stage
$R_{i,t}^{dw/up,g}$	Ramp down/up reserve provided by dispatchable generation unit i at time t in the first stage
$R_t^{dw/up,c}$	Ramp down/up reserve provided by utility grid through the point of common coupling at time t in the second stage

I. INTRODUCTION

Microgrids are becoming one of the most promising platforms to enable the large-scale adoption of renewable energy resources and dispatchable generators. By integrating distributed energy resources (DERs), active loads, and other smart elements into a localized self-contained network [1], microgrids represent a more flexible and secure operation paradigm that offers benefits such as higher power system resiliency [2], lower distribution cost [3], and improvement of rural electrification [4].

Microgrids are constantly exposed to uncertainties from components and operational environments [5]-[6]. The outputs of renewable generation in microgrids is a major source of uncertainties due to their highly volatile and stochastic nature. Another major type of uncertainties comes from the microgrid operation mode switching. A grid-connected microgrid can switch to island mode to maintain uninterrupted functioning when there is a disturbance in the upstream distribution network such as nature disasters [7] or

cyber-attacks [8]. It can switch back to grid-connected mode and resynchronize with the utility grid (i.e. main grid) when the disturbance is cleared [7]. Such disturbances are often random events, which commonly cause deviations from the day-ahead islanding schedule, i.e., start time and its duration [9]. The power fluctuations resulted from these two sources of uncertainties introduce a significant risk in microgrid operation and may negatively impact the power balance within the microgrid. When a microgrid is connected to the main distribution network, this issue is less critical as the main grid can provide continuous support to help mitigate power mismatches in the microgrid. However, following the operation mode switching from grid-connected to islanded, the original power balance within a microgrid can be severely disturbed as the interaction between the microgrid and the main grid is forced to zero [10]. Given the limitation of size and capacity of synchronous generation in a microgrid, as well as the stressed stability margin [11][12], such large sudden power imbalances would lead to drastic frequency fluctuations, e.g., a frequency deviation at the rate of 10 Hz/second as reported in [13], and even system-wide failures due to low system inertia. Therefore, the continuous balancing of resources and load within the microgrid needs to be tightly enforced to maintain the system frequency at its target value and ensure the stability of the microgrid during normal and abnormal operating conditions.

To facilitate the flexible integration of variable energy sources and stable microgrid operation [14], incorporating ancillary services to address frequency instability caused by uncertainties becomes a natural choice for microgrid operators [15]. Existing literature shows that market-based ancillary services can be exchanged on an hourly basis in the day-ahead market and provide a reliable, effective, and flexible way to maintain power balance between generation and demand, and limit system frequency excursions in real-time [15]-[18]. For the consideration of microgrid frequency stability, a certain amount of active power, commonly referred to as *frequency control reserve* (FCR), can be procured by the microgrid operator (MGO) [16] to respond immediately to potential system frequency deviations from the target value and provide the reserve capacity required to fulfill the operational requirement within a short period of time [17][18]. Under the assumption that a joint energy and ancillary services market [19] is available to the microgrid on the distribution system level, the MGO can (i) purchase fast-reacting FCR services as commodities from the main grid in grid-connected mode; (ii) prepare its own self-sustaining FCR provided by internal dispatchable units equipped with droop-based control for fast frequency regulation. Regardless of which approach the MGO takes, the operation uncertainties from supply/demand and microgrid operation mode switching, as well as the tradeoff between mitigating the risk of losing stability using ancillary services and the increased operation costs resulted from the reserve preparation needs to be analytically examined as a decision-making problem for MGO during scheduling.

Although microgrid operation scheduling has been extensively investigated in the literature, the research on microgrid scheduling incorporating both ancillary services and islanding has been limited. The primary drawback of current approaches is that the impact of operation mode switching is not adequately addressed in the scheduling

process, which oversimplifies the scheduling problem to a scaled-down unit commitment problem. Such a scheme considers island mode [20]–[23], and grid-connected mode [10], [24], without including the transition [15] in between. This is highly problematic for low-inertia systems such as microgrids as unexpected operation mode switching can be a major source for frequency deviations and ancillary services has to be adequately scheduled and readily deployable by the MGO when the islanding occurs. Notable literature such as [10] and [15] has attempted to systematically address the reserve provision for islanding events in microgrid scheduling in a joint market environment. A responsible party rule was provided in [15] which suggested that a microgrid can switch to island mode when the procured reserve band that can be purchased from the market cannot handle the frequency deviation. However, the provision of reserve before and after islanding are not considered. Another case in [10] shows that a microgrid is required to have enough reserve capacity to handle the power mismatch when it switches from grid-connected mode to island mode; nonetheless, the reserve providers are not clearly identified and the scheduling strategy for the duration of islanding is not discussed. A truly comprehensive scheduling scheme that incorporates the full process of the islanding event to assure the seamless transition between grid-connected mode and island mode is still yet to be developed.

Realizing the limitations of the previous research efforts, in this paper, a novel two-stage microgrid scheduling strategy is proposed to facilitate the economic and stable operation of a microgrid that participates in the joint distribution market. To the best of our knowledge, this is a pioneering work on addressing the optimal scheduling of a microgrid with the full incorporation of market-oriented frequency control reserve scheduling and the transition between operation mode switching. While our goal for the proposed scheduling strategy is to produce the most cost-effective solution without violating any power balance constraints (i.e., frequency stability constraints), such a solution can be very difficult and costly to obtain in the face of uncertainties. Therefore, the authors argue that a certain degree of frequency stability constraint violation can be tolerated as long as the frequency deviation caused by such power mismatch is within a certain range at a cost, e.g., 59.3 Hz to 60.5 Hz, according to IEEE Std 1547.4 for a 60 Hz system [25]. This motivates us to formulate the microgrid operation scheduling problem in the form of chance-constrained programming (CCP) [26] where the frequency stability violation can be conveniently captured in the form of chance constraints that only need to be satisfied with a probability. However, the violation of such constraints will be susceptible to penalties when the system frequency exceeds the desired bounds, and load shedding or power curtailments are required to mitigate the power mismatch and maintain system stability. Through optimization, the proposed scheduling algorithm is seeking the complementary between frequency control reserve, as a service to ensure microgrid stability, and energy supply, which is cost-driven.

The detailed contributions of this paper are described as follows:

1. A two-stage microgrid scheduling strategy is proposed based on CCP that allows the MGO to pursue its own economic interest of minimizing the operational cost of the

microgrid while actively mitigating the risk of system instability within the scheduling horizon under uncertainty.

2. Islanding events along with the uncertainties associated with them are fully considered. The proposed scheduling strategy takes into account all states of microgrid operation including grid-connected, islanded, and the transition in between. Ancillary services providers and guidelines for reserve preparation are defined end-to-end to assure sufficient resources are allocated and ready for power imbalances.

3. A collaborative resource allocation strategy is formulated in the proposed scheduling framework to determine the proper amount of reserve from market purchase and internal preparation, respectively. This allows us to achieve another level of co-optimization on top of the energy and reserve co-optimization that is originally offered in the joint market.

4. Policy studies are performed to evaluate the proposed microgrid scheduling strategy in terms of both operation economics and stability requirement.

The remainder of this paper is organized as follows. Section II presents the proposed microgrid management strategy. Section III formulates the chance-constrained programming model and our proposed solution methodology. The model is tested under different operation scenarios and policy settings in Section IV. Conclusions are drawn in Section V.

II. MICROGRID MANAGEMENT STRATEGY

A. Joint market environment

In a fully decentralized market environment, successful microgrid operation scheduling requires coordination with the electricity distribution market [27]. The participation of microgrids in a distribution level day-ahead electricity market by providing both energy and ancillary services such as reactive power/voltage control, active loss balancing and demand interruption was first discussed in [28] and [29]. The interfacing mechanisms of microgrids with ancillary services markets cleared by distribution system operator were systematically investigated and discussed in [30]. Algorithms to enable regulation and primary control service for individual and multiple microgrids have been reported [31] and [32]. Readers can find a collective review and discussion of the types and quantification of ancillary service provision by microgrid [33]. As a participant of a competitive market, literature [34]–[37] have evaluated the optimal bidding strategy for microgrids in day-ahead and real-time joint energy and ancillary services markets to maximize the revenue and facilitate flexible integration of renewable DERs into the utility grid.

This paper adopts the *power exchange for frequency control* (PXFC) market structure [38] as it provides a competitive and transparent market environment for participants to make individual decisions regarding the purchase quantities, purchase costs, as well as the risk for utilizing unreserved energy. The PXFC market consists of two submarkets: an energy market and a reserve market [15]. In the energy market, reference power is traded based on anticipated internal power generation and demand within the microgrid. In the reserve market, a bandwidth around the reference power is exchanged among market participants. This bandwidth, known as *frequency control band*, can be used as the reserved capacity of FCR to compensate for

deviations from the expected reference power. By combining the reference power and the frequency control band, an *external reserve band* can be defined as:

$$\Gamma_1 = \psi_1 \pm \theta_1 \quad (1)$$

where, ψ_1 denotes the reference power and θ_1 denotes the width of the frequency control band. It is clear that Γ_1 can be entirely purchased by the MGO from the joint market.

However, the external reserve band Γ_1 by itself cannot guarantee the stable operation of the microgrid, as such reserve market will become unavailable to microgrid during the islanding operation. Therefore, the MGO needs to prepare its own operation reserve band to regain power balance and maintain system stability in island mode. Inverter-based dispatchable units can provide a fast response to frequency deviations in the form of *internal reserve band* Γ_2 . Similar to the external reserve band, Γ_2 consists of an internal reference power ψ_2 and an internal frequency control bandwidth θ_2 :

$$\Gamma_2 = \psi_2 \pm \theta_2 \quad (2)$$

Considering the high operation cost associated with the dispatchable units, the MGO should be very careful in allocating the limited generation capacity of a microgrid for energy supply and internal reserve preparation. With Γ_1 and Γ_2 both contributing to the total energy and FCR provision in the form of a combined FCR band of Γ (i.e. $\Gamma = \Gamma_1 + \Gamma_2$), a collaborative scheme is critical to schedule both Γ_1 and Γ_2 simultaneously to improve the scheduling efficiency and effectiveness. A two-stage scheduling process is proposed to achieve this goal in the proposed market environment. Considering the relatively small capacity of a microgrid, it is assumed that Γ_2 is not traded back to the main grid in this paper.

B. Two-stage scheduling strategy

The determination of the reserve band can be divided into two major stages: (i) *band preparation* and (ii) *band verification*. In the first stage, the MGO determines the amount of energy and FCR to prepare for the operation of the microgrid as well as the uncertainties that may occur in real-

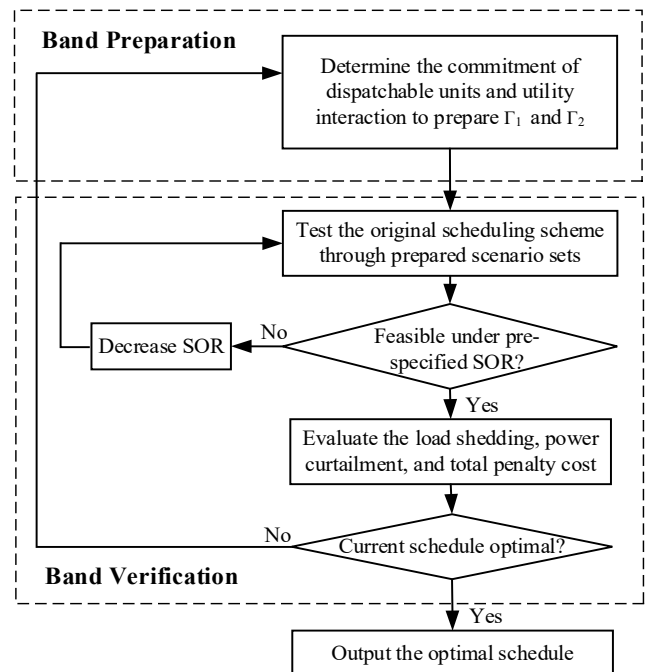


Fig. 1. Decision Flow Using SOR

time through adjusting the combination of Γ_1 and Γ_2 . The second stage is to test the total bandwidth requested in the first stage. A large number of scenarios need to be tested to verify whether the bandwidth requested is sufficient to maintain the stable operation of the microgrid under various types and severities of operation uncertainties. The performance of these tests can then be submitted to a supervisory authority that oversees the microgrid operation to determine the penalty for power balance violation that may lead to load shedding (LS) or power curtailment (PC). The penalties are imposed to encourage the MGO to purchase a proper bandwidth in the first stage.

The connection between the first and second stage is the width of the reserve band. A wide bandwidth indicates a higher cost because more reserve will be scheduled to ensure stability, which is a typical decision preference of conservative decision makers, i.e., risk-averse in the context of decision analysis. Conversely, a narrow bandwidth means lower preparation cost, but it also increases the risk of system instability and the penalty cost resulted from load shedding and power curtailment, which is preferred by aggressive decision makers, i.e., risk-prone. To capture these differences in risk-behavior of the MGOs and provide a mathematical tool reflecting their risk level ($\varepsilon \in (0,1]$), the authors propose the concept of chance-constraints [39] that allows constraint violation up to the level of pre-specified ε , which is called the confidence level. Note that one can convert a set of constraint $Ax \leq b$ to a chance constraint $\text{Prob}(Ax \leq b) \geq 1 - \varepsilon$. In this work, the confidence level ε is referred to as *stability opportunity risk (SOR)* to represent the MGO's risk preference. Hence, our proposed model incorporating the user-defined parameter SOR can be stated in the following form:

$$\text{Prob}(\text{No LS or PC required}) \geq 1 - \text{SOR} \quad (3)$$

Eq. (3) clearly indicates that SOR, as a risk measure, represents the level of the MGO's confidence in satisfying the stability constraint under uncertainty. Incorporating the concept of SOR, the proposed two-stage process is depicted in Fig. 1. Note that in the second stage, the MGO needs to iteratively adjust its SOR setting, if necessary, to ensure the feasibility of optimal solution under the prepared scenarios representing possible microgrid operation uncertainties.

Another critical issue that needs to be taken into consideration in the proposed two-stage process is the switching of both the reserve band providers and the width of the reserve band before and after islanding. This is addressed in the following section where a set of islanding rules are outlined.

C. Islanding Rules

As indicated in [15], the successful implementation of a PXFC market requires enforcement and penalty to assure participants do not misrepresent their load/generator characteristics (i.e., wrong width for the reserve band). This is especially true for microgrid operation around islanding events, since the type of reserve, the responsible parties of reserve provision, and the width of the reserve band all alter with the operation mode switching. For the purpose of microgrid scheduling, the following islanding rules are adopted:

Rule I: In grid-connected mode, the MGO purchases FCR from the main grid for frequency regulation.

Comment: In grid-connected mode, only external reserve

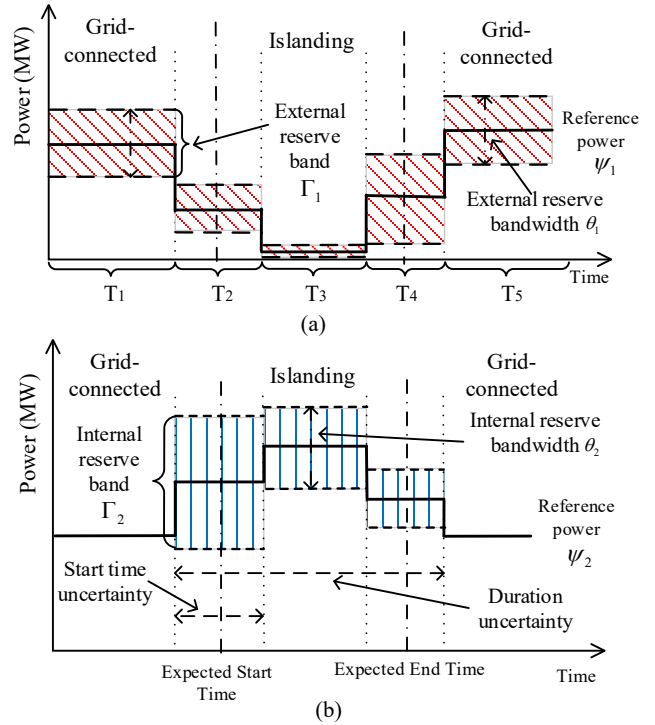


Fig. 2. External and Internal Reserve Band

band Γ_1 is used because the frequency of the microgrid is dominantly determined by the main grid. The FCR purchased are primarily used to provide frequency regulation for uncertainty associated with DER and load variations.

Rule II: When the microgrid approaches the anticipated islanding start time, the MGO starts to lower the amount of market purchase and prepare internal FCR for the upcoming islanding event.

Comment: During this time window, while the MGO still purchases a portion of Γ_1 from the main grid, it primarily relies on establishing Γ_2 to mitigate the large power mismatch caused by the upcoming islanding event.

Rule III: During the islanding event, the MGO fully relies on its own internal FCR for the frequency regulation.

Comment: Once the microgrid fully enters into island mode and starts stable operation, the interactions between the main grid and the microgrid are paused. Only Γ_2 provided by dispatchable units within the microgrid can be used to mitigate frequency deviations.

Rule IV: When microgrid is approaching the anticipated islanding end time, the MGO starts to lower the amount of internal FCR for the upcoming reconnection to the main grid.

Comment: Similar to Rule II, during this time interval, the MGO needs to reduce Γ_2 as once reconnected to the main grid, the power mismatch will be primarily handled by Γ_1 to be purchased from the main grid.

Rule V: The penalty for the stability constraint violation in grid-connected mode is lower than that for island mode.

Comment: As a rule of thumb, grid-connected microgrid is allowed to take more risk as it has continuous support from the main grid. On the contrary, during island mode, the MGO has limited resources with no main grid backup. A higher penalty cost is thus used to discourage the MGO from taking risks.

A representative case describing the change of reserve provision incorporating the proposed islanding rules is shown in Fig. 2, which includes external reserve band (a) and internal reserve band (b). The whole islanding process can be divided into five phases denoted by time interval T_1 through

T_5 in the figure. Prior to the operation mode switching, microgrid is in grid-connected mode during T_1 . Due to uncertainties associated with the islanding start time, for the purpose of operation scheduling, the transition from grid-connected mode to island mode takes up-to a time duration of T_2 to complete. Then, the microgrid enters the stable islanding operation that lasts a duration of T_3 . Once the microgrid is ready to be reconnected to the main grid, the transition back to grid-connected mode takes a period of time T_4 to complete considering the islanding duration uncertainty. The microgrid is fully back to grid-connected mode in T_5 .

By comparing the bandwidth of Γ_1 and Γ_2 for different stages in (a) and (b), it can be observed that for this particular example, the bandwidth of Γ_1 in T_1 is consistent with the bandwidth of Γ_1 during T_5 and the bandwidth of Γ_2 during T_3 . This is because according to Rule I and III, the reserve band mainly serves the need of frequency regulation for DERs during those time intervals. Rule II applies to period T_2 , in which the bandwidth of Γ_1 is narrower than Γ_2 as microgrid is primarily responsible for the provision of FCR for the anticipated upcoming islanding event. Similarly, based on Rule IV the bandwidth of Γ_2 during T_4 is narrower than Γ_1 since now it is the responsibility of the main grid to provide sufficient bandwidth to handle the uncertainties associated with reconnection. Note that Γ_1 and Γ_2 are both scheduled during T_2 and T_4 due to the probabilistic nature of the proposed scheduling approach. For actual operation, once disconnected from the main grid, a microgrid loses its access to Γ_1 from the main grid immediately and this transition is instantaneous.

III. MODEL AND METHOD

A. Two-stage chance-constrained programming model

As previously discussed, the optimal scheduling problem described in Section II can be formulated as a two-stage chance-constrained programming model, in which the first-stage problem is formulated as follows:

$$\begin{aligned} \min \sum_{i,t} (c_i^g q_{i,t}^g + x_{i,t} SU_i + y_{i,t} SD_i + c_i^r (R_{i,t}^{up}, R_{i,t}^{dw})) \\ + \sum_t (\rho_t^c q_t^c + \rho^r (R_t^{up,c}, R_t^{dw,c})) \end{aligned} \quad (4)$$

The objective function (4) is to minimize the total operation cost of a microgrid which consists of dispatchable generation operation cost and interaction cost at the point of common coupling (PCC). More specifically, the generator operation cost is composed of power generation cost, startup cost, shutdown cost, and cost of the generation reserve preparation [40]. The interaction cost includes power interaction cost (negative if power is transferred from the microgrid to the utility) and ancillary services purchase cost. For simplicity, all the reserve cost functions c_i^r and ρ^r are defined as linear functions of variable $R_{i,t}^{up}, R_{i,t}^{dw}, R_t^{up,c}, R_t^{dw,c}$ as shown in (4) in this paper.

As a general rule of thumb, all the dispatchable units within the microgrid are subject to power capacity constraints (5), minimum uptime (6) restrictions, and minimum downtime restrictions (7) as follows:

$$b_{i,t} q_i^{g,\min} \leq q_{i,t}^g \leq b_{i,t} q_i^{g,\max} \quad \forall i \in D, \forall t \quad (5)$$

$$(X_{i,t}^{on} - T_i^{on}) * (b_{i,t-1} - b_{i,t}) \geq 0 \quad \forall i \in D, \forall t \quad (6)$$

$$(X_{i,t-1}^{off} - T_i^{off}) * (b_{i,t} - b_{i,t-1}) \geq 0 \quad \forall i \in D, \forall t \quad (7)$$

Under the assumption that all the dispatchable units can provide both ramp-up and ramp-down reserve, their reserve capacity limits can be described by (8) and (9).

$$0 \leq R_{i,t}^{up,g} \leq R_i^{up,\max} b_{i,t} \quad \forall i \in D, \forall t \quad (8)$$

$$0 \leq R_{i,t}^{dw,g} \leq R_i^{dw,\max} b_{i,t} \quad \forall i \in D, \forall t \quad (9)$$

The output capacity and ramp-up/down capability are limited by both physical characteristics and reserve capacities of the each dispatchable unit as shown in (10)-(13).

$$q_{i,t}^g + R_{i,t}^{up,g} \leq q_i^{g,\max} \quad \forall i \in D, \forall t \quad (10)$$

$$q_{i,t}^g - R_{i,t}^{dw,g} \geq q_i^{g,\min} \quad \forall i \in D, \forall t \quad (11)$$

$$q_{i,t}^g - q_{i,t-1}^g + R_{i,t}^{up,g} \leq (2 - b_{i,t-1} - b_{i,t}) q_i^{g,\min} + (1 + b_{i,t-1} - b_{i,t}) RU_i \quad \forall i \in D, \forall t \quad (12)$$

$$q_{i,t-1}^g - q_{i,t}^g - R_{i,t}^{dw,g} \leq (2 - b_{i,t-1} - b_{i,t}) q_i^{g,\min} + (1 - b_{i,t-1} + b_{i,t}) RD_i \quad \forall i \in D, \forall t \quad (13)$$

In a joint market environment, the interaction between the microgrid and the main grid includes power that flows both ways and external reserve that flows from main grid to the microgrid. The power interaction has upper/lower bounds as shown in (14) considering the physical limit of the PCC.

$$q^{c,\min} \leq q_t^c \leq q^{c,\max} \quad \forall t \quad (14)$$

The ramp-up external reserve and ramp-down external reserve capability offered by the main grid also have upper/lower limits as shown in (15) and (16).

$$0 \leq R_t^{dw,c} \leq R^{dw,c,\max} \quad \forall t \quad (15)$$

$$0 \leq R_t^{up,c} \leq R^{up,c,\max} \quad \forall t \quad (16)$$

Combining the power exchange and external reserve procurement, the total interaction between the microgrid and the main grid needs to be within the physical limit imposed by the PCC at all time.

$$q_t^c + R_t^{up,c} \leq q^{c,\max} \quad \forall t \quad (17)$$

$$q_t^c - R_t^{dw,c} \geq q^{c,\min} \quad \forall t \quad (18)$$

The power balance equation (19) ensures that the power generation from dispatchable and non-dispatchable units within the microgrid, together with the power exchange with the main grid, can supply the local demand of the microgrid.

$$\sum_i q_{i,t}^g + \sum_j q_{j,t}^w + q_t^c = \sum_k l_{k,t} \quad \forall t \quad (19)$$

The second stage model presents the determination of the risk penalty with the specification of different operation uncertainties scenarios as follows:

The objective function of the second stage problem is to minimize load shedding and power curtailment in both island mode and grid-connected mode as shown in (20).

$$\min \sum_{s,t} \left(\alpha_t * (VOPC \cdot I_{s,t}^{sh} + VOLL \cdot q_{s,t}^{cu}) * I_{s,t}^{grid} + \beta_t * (VOPC \cdot I_{s,t}^{sh} + VOLL \cdot q_{s,t}^{cu}) * I_{s,t}^{island} \right) \quad (20)$$

Note that according to Rule V, the penalty coefficient α associated with island mode is higher than that of grid-connected mode β .

The chance constraints are used to demonstrate the effects of using external and internal reserve to handle frequency instability caused by power mismatch at two tails. Particularly, if the total ramp-up reserve is insufficient to supply the load, load shedding will occur. Incorporated the previously defined concept of *SOR*, this chance constraint is shown in (21).

$$\begin{aligned} & \text{Prob}\left(\sum_i q_{i,t}^g + \sum_j q_{j,t,s}^w + q_{s,t}^c + \sum_i r_{i,t,s}^{up,g} + r_{t,s}^{up,c} \geq \sum_k l_{k,t,s}\right) \\ & \geq 1 - \text{SOR}_1 \quad \forall t, \forall s \end{aligned} \quad (21)$$

If the total ramp-down reserve is insufficient to decrease the excessive generation, power curtailment will occur. Similarly, this chance constraint is shown in (22)

$$\begin{aligned} & \text{Prob}\left(\sum_i q_{i,t}^g + \sum_j q_{j,t,s}^w + q_{s,t}^c - \sum_i r_{i,t,s}^{dw,g} - r_{t,s}^{dw,c} \leq \sum_k l_{k,t,s}\right) \\ & \geq 1 - \text{SOR}_2 \quad \forall t, \forall s \end{aligned} \quad (22)$$

In this work, it is assumed that for the MGO's risk preference for load shedding (i.e. SOR_1) and generation curtailment (i.e. SOR_2) are equal. However, (21) and (22) are formulated in a generalized way to accommodate different risk preference settings easily when needed.

Following the possible load shedding and power curtailment operation, the power balance of the microgrid still needs to be strictly ensured as shown in (23). Constraint (24) ensures the validity of the load shedding and power curtailment operation.

$$\begin{aligned} & \sum_i q_{i,t}^g + \sum_j q_{j,t,s}^w + q_{s,t}^c + \sum_i r_{i,t,s}^{up,g} + r_{t,s}^{up,c} - \\ & \sum_i r_{i,t,s}^{dw,g} - r_{t,s}^{dw,c} - q_{s,t}^{cu} = \sum_k l_{k,t,s} - I_{s,t}^{sh} \quad \forall t, \forall s \end{aligned} \quad (23)$$

$$I_{s,t}^{sh} \geq 0, q_{s,t}^{cu} \geq 0 \quad \forall t, \forall s \quad (24)$$

A noticeable effect caused by operation mode switching is that the interaction with the main grid, including the access to external reserve, will disappear immediately after the microgrid switches to island mode. For this purpose, binary indicators $I_{s,t}^{grid}$ is introduced to indicate if the microgrid is in grid-connected mode (i.e. $I_{s,t}^{grid} = 1$) or island mode (i.e. $I_{s,t}^{grid} = 0$). It is evident the power interaction only exists when microgrid is working on grid-connected mode as depicted in (25).

$$q_{s,t}^{c,max} I_{s,t}^{grid} \leq q_{s,t}^c \leq q_{s,t}^{c,max} I_{s,t}^{grid} \quad \forall t, \forall s \quad (25)$$

Similarly, the external reserve can only be accessed when the microgrid is in grid-connected mode based on Rule I as shown in (26) and (27).

$$0 \leq r_{t,s}^{up,c} \leq R_t^{up,c} I_{s,t}^{grid} \quad \forall t, \forall s \quad (26)$$

$$0 \leq r_{t,s}^{dw,c} \leq R_t^{dw,c} I_{s,t}^{grid} \quad \forall t, \forall s \quad (27)$$

According to Rule I, when the microgrid is in grid-connected mode, no internal reserve is required. Introducing the complementary binary parameter $I_{s,t}^{island}$, this setting can be represented as follows:

$$0 \leq r_{i,t,s}^{up} \leq R_{i,t}^{up} I_{s,t}^{island} \quad (28)$$

$$0 \leq r_{i,t,s}^{dw} \leq R_{i,t}^{dw} I_{s,t}^{island} \quad (29)$$

B. Scenario generation

Two types of operational uncertainties are considered in this paper: forecast error and operation mode switching. More specifically, normal distribution is adopted to describe the forecast errors of renewable energy output and hourly load consumption. The probability distribution of renewable energy output and hourly load forecast is given as follows:

$$q_{j,t,s}^w \square N(W_{j,t}^0, \sigma_{j,t}^w) \quad \forall j, \forall t \quad (30)$$

Scenario #	Starting Time	Duration
1	11.583	1.962
2	12.936	3.216
3	8.781	2.303
4	11.938	2.383
...
N-1	12.424	3.657
N	11.753	1.809

Round to integer as 12 and 2.

Time Slot t	1	11	12	13	14	24
Grid-connected $I_{s,t}^{grid}$	1	1	0	0	1	1
Islanding $I_{s,t}^{island}$	0	0	1	1	0	0

Fig. 3. Generating operation mode scenarios

$$l_{k,t,s} \square N(L_{k,t}^0, \sigma_{k,t}^l) \quad \forall k, \forall t \quad (31)$$

The forecast error from renewable energy output and hourly load may have certain correlations for long-term microgrid planning. However, it is assumed that renewable energy output and load are independent from each other because such correlations are not significant for short-term operation (day-ahead) as studied in this paper [41].

For indicator $I_{s,t}^{island}$ and $I_{s,t}^{grid}$ that represent the operation mode switching, a total of $N \times T$ scenarios is considered in the scheduling process. Based on the proposed islanding rules, two types of information are required: start time μ and time duration v . While the microgrid operator can make reasonable forecasts that the microgrid mode switching is expected to occur at time $\bar{\mu}$ for \bar{v} hours, this forecast may not be accurate. If the probability distributions of μ and v are independent of each other, a data set can be generate which contains start time and duration first, then convert it to binary indicators. Due to the lack of data in the occurrence and duration of disturbances that may lead to islanding, normal distribution is used to represent the islanding scenarios. The probability distribution functions of occurrence and duration are thus approximated as discrete scenarios so that it can be conveniently used in the proposed optimization model. More specifically, it is assumed that

$$\mu \square N(\bar{\mu}, \sigma_{start}^2) \quad (32)$$

$$v \square N(\bar{v}, \sigma_{duration}^2) \quad (33)$$

The process of generating islanding scenarios is illustrated in Fig. 3. To begin with, a set of start time and duration data is generated based on probability distributions. Then, for each scenario, the sampling numbers are rounded to integers, so that a series of binary grid-connected indicators and islanding indicators can be generated to indicate the operation mode of a microgrid at a certain time slot within the scheduling horizon. These indicators are used later in the model as parameters.

The *Latin Hypercube Sampling* method is applied to generate N scenarios for stochastic variables. Each scenario has the same probability, thus the second stage objective function (20) can be replaced by:

$$\min \frac{1}{N} \sum_N \sum_{s,t} \left(\alpha_t * (VOPC \cdot I_{s,t}^{sh} + VOLL \cdot q_{s,t}^{cu}) * I_{s,t}^{grid} + \beta_t * (VOPC \cdot I_{s,t}^{sh} + VOLL \cdot q_{s,t}^{cu}) * I_{s,t}^{island} \right) \quad (34)$$

C. Approximation

After scenario generation, the chance constraints are still difficult to solve since they are not convex. Hence, the chance constraints are approximated as mixed-integer constraints which are easier to solve, by introducing ancillary

binary decision variable z . For a given sample size N : for each n , if $z_n = 0$, it means that the chance constraint is feasible in this scenario; if $z_n = 1$, the corresponding chance constraint is not feasible. The chance constraints are thus equivalent to limiting the number of z_n , where $1 \leq n \leq N$. Then, the chance constraints (21) and (22) can be approximated as follows:

$$\sum_i q_{i,t}^g + \sum_j q_{j,t,s}^w + q_{i,t}^c + \sum_i r_{i,t,s}^{up,g} + r_{t,s}^{up,c} - \sum_k l_{k,t,s} \geq z_n^{shed} O \quad \forall t, \forall s \quad (35)$$

$$\sum_{n=1}^N z_n^{shed} \leq N \cdot SOR_1 \quad (36)$$

$$\sum_i q_{i,t}^g + \sum_j q_{j,t,s}^w + q_{i,t}^c - \sum_i r_{i,t,s}^{dw,g} - r_{t,s}^{dw,c} - \sum_k l_{k,t,s} \leq z_n^{curl} O \quad \forall t, \forall s \quad (37)$$

$$\sum_{n=1}^N z_n^{curl} \leq N \cdot SOR_2 \quad (38)$$

The mixed-integer linear programming model can be derived by combining the first stage objective function (4) and second stage objective function (36) together as:

$$\begin{aligned} & \min \sum_{i,t} (c_i^g q_{i,t}^g + x_{i,t} S U_i + y_{i,t} S D_i + c_i^r (R_{i,t}^{up}, R_{i,t}^{down})) \\ & + \sum_t \rho^c q_t^c + \rho^r (R_t^{up,c}, R_t^{down,c}) \\ & + \frac{1}{N} \sum_{n=1}^N (\sum_{s,t} \alpha_n * (VOPC \cdot I_{s,t}^{sh} + VOLL \cdot q_{s,t}^{cu}) * I_{s,t}^{grid} \\ & + \beta_n * (VOPC \cdot I_{s,t}^{sh} + VOLL \cdot q_{s,t}^{cu}) * I_{s,t}^{island}) \end{aligned} \quad (39)$$

$$s.t. \quad (5)-(19) \quad (40)$$

$$(23)-(29), (35)-(38)$$

IV. NUMERICAL EXPERIMENTS

The model derived in (39) and (40) is evaluated based on a microgrid with five dispatchable units, one solar generator, one wind generator, and one aggregate load. It is assumed that all dispatchable units are equipped with droop-control loops to provide fast ramp rates for frequency regulation. The detailed specifications of the microgrid and the utility grid it interacts with can be found in Table I-V in the Appendix. Additional market configurations considered in case studies can be found in Table VI-VIII including fixed penalty price, market-based penalty price, and market price.

The scheduling problem was solved using IBM CPLEX [42] on a computer equipped with 2.80 GHz Intel CPU and 8GB of RAM. To evaluate the proposed scheduling strategy, the following two sets of policy studies are performed.

A. Operation policy study

In the first study, we conduct a set of experiments using different parameters including islanding scenarios, penalty price, reserve price, reserve capacity, and SOR to evaluate how the proposed scheduling approach performs under different operation settings. Four most representative cases are presented to illustrate our findings.

Policy I: Grid-connected microgrid operation without islanding

Policy II: Microgrid operation with operation mode switching

Policy III: Microgrid operation with operation mode switching under market-based penalty

Policy IV: Microgrid operation with operation mode switching and increased maximum allowable reserve band

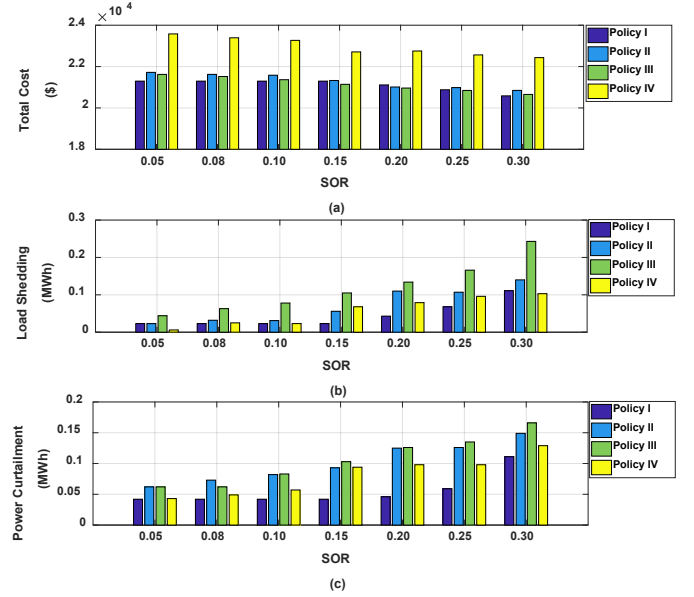


Fig. 4. Results of different operation policies under different SORs

Selected results are shown in Fig.4, which include the total operation cost (a), load shedding (b) and power curtailment (c) for the microgrid with regards to different SORs under different policies. Note that the same operation mode switching scenario is used in Policy II, III and IV for consistency whereas the islanding is expected to occur at 5:00 am with a duration of three hours. It is assumed that the deviations of the islanding start time μ and islanding duration v can be modeled using the standard normal distribution with a mean value of 0 and a variance of 1 hour.

A general trend shown in Fig.4 for all policies studied is that with an increased SOR, the operational cost decreases while the load shedding and power curtailment increase. This observation matches our trade-off analysis during the two-stage design in Section II. B. As a representative case, the external reserve band under two different levels of SOR is compared in Fig. 5 for Policy I. It can be clearly observed that when the SOR is lower, the reserve bandwidth is substantially wider which indicates that more reserve will be procured by the MGO to handle operation uncertainties since the MGO is more risk-averse. Conversely, for a risk-prone MGO that prefers a greater SOR in favor of reducing cost under uncertainty, less reserve will be procured.

To study the impact of islanding on the scheduling strategy under the same SOR, the simulation results from Policy I and Policy II are compared. In Policy I, there is no expected islanding for the scheduling period, while in policy II, an islanding event is considered. It can be observed that compared to Policy I, Policy II has a higher operation cost under the same SOR level, since expensive dispatchable units within the microgrid have to be deployed by the MGO to prepare the microgrid's internal reserve to handle the potential islanding.

The external and internal reserve band derived from Policy

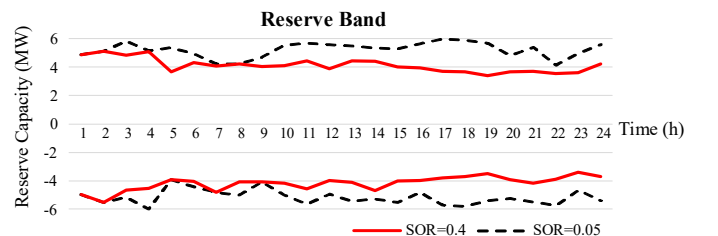


Fig. 5. Width of the External Reserve Band for Policy I under different SORs

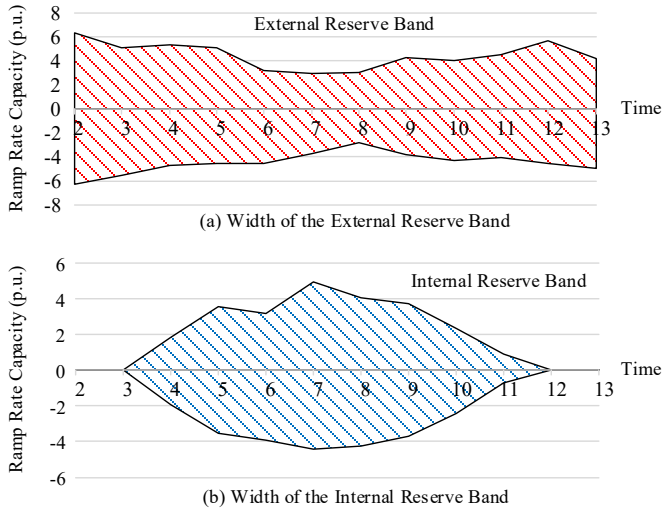


Fig. 6. Width of the External/Internal Reserve Band for Policy II

II is shown in Fig. 6 when $SOR=0.3$. As the figure depicts, the external reserve band starts to shrink, and the internal reserve band starts to appear at 3:00 am due to the uncertainty associated with islanding start time. This observation matches islanding rule II as described in Section II.C. While the islanding is expected at 5:00 am, it will most likely occur any time within the time span between 3:00 am to 7:00 am based on the scenario generation process described in Section III.B. Between 5:00 am to 8:00 am, the bandwidth of the internal reserve is kept at a high level as according to islanding rule III, the MGO is now fully relying on it to handle operation uncertainties. Conversely, only limited external reverse bandwidth needs to be retained during this time period as the MGO may lose access to the utility grid during this period of time caused by islanding. Due to the uncertainty associated with the duration of the islanding, between 8:00 am to 11:00 am, the internal reserve band becomes narrower as the islanding end time is approaching, and the MGO starts to switch back to the external reserve. As shown in Fig. 6 (b), the internal reserve band completely disappears at 12:00 pm. It can also be observed that the external and internal reserve bands are not symmetrical in ramp-up and ramp-down capacity. For this experiment setting, the ramp-up reserve is always greater because the penalty associated with load shedding is commonly higher than power curtailment (see Table. IV in the Appendix). Another noticeable difference between Policy I and II is that, despite the increased operation cost, Policy II tends to result in higher load shedding and power curtailment. This suggests that although the internal reserve provided by dispatchable units helps mitigate the power mismatch during islanding, the microgrid still faces higher operational risk due to the loss of support from the utility grid.

Policy II can also be compared with Policy III where a market-based penalty price is adopted which has a similar trend as the fluctuation of market price (see Table. VII in the Appendix). It can be clearly observed that Policy III has significant higher load shedding and power curtailment with a slight decrease in total cost. This effect can be traced back to the penalty price during the expected islanding event. Since such event is expected to occur during non-peak hours during which the penalty prices are low, the MGO tends to take higher risk and accept penalty for cost-benefit consideration under this market configuration, which directly results in the high amount of power curtailment and load shedding. This motivates us to conduct more experiments to

evaluate the positive and negative influence of prices, including penalty price and reserve price, on power curtailment and load shedding. It is found out that as a general trend, an increased penalty price can help reduce load shedding and power curtailment, but the effects are not significant. Similarly, results from the reserve price experiments show that a reduced reserve price has slightly positive effects on reducing load shedding and power curtailment, to a certain degree. This indicates that for a given SOR, while an increased penalty price/a reduced reserve price encourages the MGO to purchase more reserve, this effect is limited. On the contrary, if a reduced penalty price is available, the MGO is more inclined to procure less reserve and thus takes more risk of load shedding and power curtailment.

A noticeable case is presented in Policy IV in which the maximum allowable external reserve bandwidth is changed from 7 MW to 8 MW. The results shown in Fig.4 indicate that the operational cost rises drastically with considerably decreased load shedding and power curtailment. This matches our discussion in Section II.B that a wider bandwidth allows the MGO to purchase a higher amount of reserve to improve the microgrid operation at a cost. Compare Policy IV to Policy II and III, it can be observed that maximum allowable reserve bandwidth, rather than the costs of reserve and penalty, is the main factor that impacts the microgrid's stability performance in terms of load shedding and power curtailment.

B. Islanding policy study

In the previous study, it is concluded that islanding events have a large impact on the scheduling results. In this section, the previous study is further expanded, and a more in-depth analysis is performed that is focused on evaluating the effects of islanding events. The following different expected islanding start time are tested:

Policy I: Islanding is expected at start at 5:00 am

Policy II: Islanding is expected at start at 10:00 am

Policy III: Islanding is expected at start at 16:00 pm

The expected start time indicate that the islanding event is expected to happen during non-peak hours (5am) for Policy I, peak hours (16:00pm) for Policy II, and in between

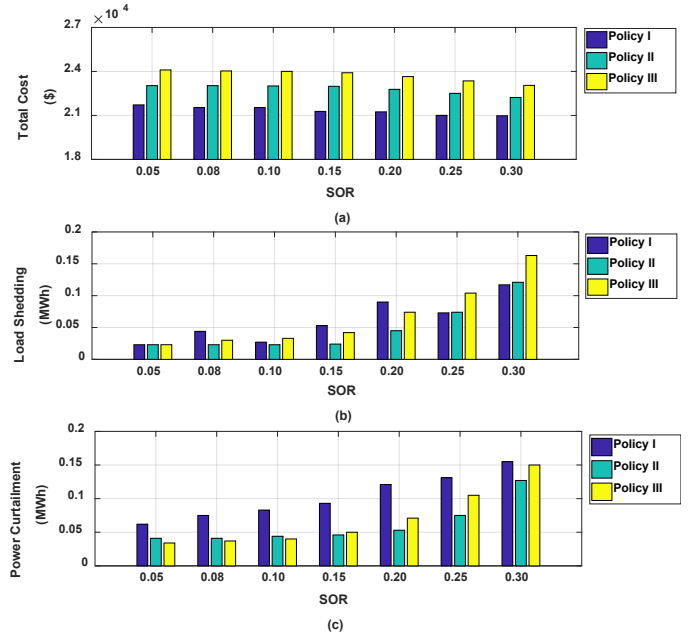


Fig. 7. Results of different islanding start time under different SORs

(10:00am) for Policy III. The expected islanding duration for these three policies are set identical (three hours). The results are presented in Fig. 7 which include total cost (a), load shedding (b), and power curtailment (c). In terms of total cost, Policy III has the highest cost, while Policy I has the lowest cost, with Policy II in the middle. This indicates that islanding during peak hours will lead to a higher operational cost because of the increased marginal cost to use dispatchable units within the microgrid. The reserve preparation also negatively affects the microgrid's power capacity to supply loads. This is especially evident for islanding during peak hours when the dispatchable units are scarcer.

Fig. 7 also shows one interesting finding in (b) and (c): the load shedding and power curtailment for islanding events occurring during the peak hours are lower than that during non-peak hours. Intuitively, the higher marginal cost to prepare reserve during the peak hour will result in a higher load shedding and power curtailment. However, it can be further investigated that despite the higher marginal cost, the amount of reserve that can be acquired during peak hours is also higher because all the dispatchable units have already been turned on. As a result, the MGO can dispatch more capacity to provide reserve since the startup cost of those dispatchable units has already been covered before the anticipated islanding starts.

The policy studies conducted in this section confirm the effectiveness of the proposed microgrid scheduling which matches previous analysis in Section II. More policy studies can be performed under our framework such as the influence of energy storage system and renewable energy profile.

V. CONCLUSIONS AND FUTURE WORK

A. Conclusion and discussion

This paper aims to bridge the current technological gaps within microgrid operation scheduling in a joint energy and ancillary services market environment with the consideration of operation uncertainties. Based on the existing concept of energy and ancillary services co-optimization, a novel two-stage microgrid scheduling approach is proposed based on CCP to allow the MGO to determine the optimal reserve preparation strategy to optimize the operational cost, increase the system efficiency while reducing the risk of system instability. Compared with previous works in the field, the proposed scheduling strategy offers a true end-to-end solution as it specifically covers all states of microgrid operation, especially, around operation mode switching, and clearly identifies the responsible parties for reserve provision as well as the amount to prepare. This is critical for microgrid scheduling as it gives the MGO sufficient capability as well as internal/external resources to handle deviations caused by uncertainties associated with forecast error and operation mode switching in real-time at the lowest cost, and thus ensures efficient, economic and reliable microgrid operation. Simulation-based policy studies are conducted based on different aspects of microgrid operation including SOR levels, price setting, capacity setting, and expected islanding event to demonstrate the effectiveness of the proposed scheduling strategy in a joint market environment.

B. Future work

As an extension to our work, one can address the effects of two simplifications adopted in the proposed scheduling

strategy through the derivation of detailed primary/secondary control strategy to enable the provision of frequency control reserve under our proposed scheduling framework. The effects of energy storage devices can also be systematically investigated. Energy storage devices such as batteries and super capacitors have insignificant direct cost for generation and start-up/shut-down compared with conventional dispatchable units, which makes them more flexible and efficient in storing and providing reserve capacities.

ACKNOWLEDGEMENT

The authors thank Dr. Masoud Barati who provided insight and expertise that assisted this research effort.

REFERENCES

- [1] N. Hatzigiorgiou, H. Asano, R. Iravani, and C. Marnay, "Microgrids," *IEEE Power Energy Mag.*, vol. 5, no. 4, pp. 78–94, 2007.
- [2] A. Khodaei, "Resiliency-oriented microgrid optimal scheduling," *IEEE Trans. Smart Grid*, vol. 5, no. 4, pp. 1584–1591, 2014.
- [3] A. Khodaei and M. Shahidehpour, "Microgrid-based co-optimization of generation and transmission planning in power systems," *IEEE Trans. Power Syst.*, vol. 28, no. 2, pp. 1582–1590, 2013.
- [4] M. Shahidehpour and S. Pullins, "Microgrids, modernization, and rural electrification [About This Issue]," *IEEE Electr. Mag.*, vol. 3, no. 1, pp. 2–6, 2015.
- [5] A. Khodaei, "Microgrid Optimal Scheduling With Multi-Period Islanding Constraints," *IEEE Trans. Power Syst.*, vol. 29, no. 3, pp. 1383–1392, 2013.
- [6] W. Su, J. Wang, and J. Roh, "Stochastic energy scheduling in microgrids with intermittent renewable energy resources," *IEEE Trans. Smart Grid*, vol. 5, no. 4, pp. 1876–1883, 2014.
- [7] L. Che, M. Khodayar, and M. Shahidehpour, "Only connect: Microgrids for distribution system restoration," *IEEE Power Energy Mag.*, vol. 12, no. 1, pp. 70–81, 2014.
- [8] L. Che and M. Shahidehpour, "Adaptive Formation of Microgrids with Mobile Emergency Resources for Critical Service Restoration in Extreme Conditions," *IEEE Trans. Power Syst.*, vol. PP, no. c, p. 1, 2018.
- [9] H. Farzin, M. Fotuhi-Firuzabad, and M. Moeini-Aghtaie, "Stochastic Energy Management of Microgrids during Unscheduled Islanding Period," *IEEE Trans. Ind. Informatics*, vol. 13, no. 3, pp. 1079–1087, 2017.
- [10] G. Liu, M. Starke, B. Xiao, X. Zhang, and K. Tomsovic, "Microgrid optimal scheduling with chance-constrained islanding capability," *Electr. Power Syst. Res.*, vol. 145, pp. 197–206, 2017.
- [11] D. E. Olivares, A. Mehrizi-Sani, A. H. Etemadi, C. A. Cañizares, R. Iravani, M. Kazerani, A. H. Hajimiragha, O. Gomis-Bellmunt, M. Saeedifard, R. Palma-Behnke, G. A. Jiménez-Estévez, and N. D. Hatzigiorgiou, "Trends in Microgrid Control," *IEEE Trans. Smart Grid*, vol. 5, no. 4, pp. 1905–1919, 2014.
- [12] Ryan, Mamay, Chris, and Firestone, "Energy manager design for microgrids," *eScholarship, University of California*, 31-Mar-2005. [Online]. Available: <https://escholarship.org/uc/item/6fm1x870>.
- [13] Q. Zhou, Z. Li, Q. Wu, and M. Shahidehpour, "Two-Stage Load Shedding for Secondary Control in Hierarchical Operation of Islanded Microgrids," *IEEE Trans. Smart Grid*, vol. 3053, no. c, pp. 1–8, 2018.
- [14] Z. Li and M. Shahidehpour, "Security-constrained unit commitment for simultaneous clearing of energy and ancillary services markets," *IEEE Trans. Power Syst.*, vol. 20, no. 2, pp. 1079–1088, 2005.
- [15] S. Y. Lee, Y. G. Jin, and Y. T. Yoon, "Determining the Optimal Reserve Capacity in a Microgrid with Islanded Operation," *IEEE Trans. Power Syst.*, vol. 31, no. 2, pp. 1369–1376, 2016.
- [16] P. a Ruiz, C. R. Philbrick, E. Zak, K. W. Cheung, and P. W. Sauer, "Uncertainty Management in the Unit Commitment Problem," *Power Syst. IEEE Trans.*, vol. 24, no. 2, pp. 642–651, 2009.
- [17] M. Q. Wang and H. B. Gooi, "Spinning reserve estimation in microgrids," *IEEE Trans. Power Syst.*, vol. 26, no. 3, pp. 1164–

- 1174, 2011.
- [18] K. W. Cheung, P. Shamsollahi, D. Sun, J. Milligan, and M. Potishnak, "Energy and ancillary service dispatch for the interim ISO New England electricity market," *IEEE Trans. Power Syst.*, vol. 15, no. 3, pp. 968–974, 2000.
- [19] S. S. Oren, "Auction design for ancillary reserve products," *Power Eng. Soc. Summer Meet. 2002 IEEE*, vol. 3, pp. 1238–1239, 2002.
- [20] Z. Shi, H. Liang, S. Huang, and V. Dinavahi, "Distributionally Robust Chance-Constrained Energy Management for Islanded Microgrids," *IEEE Trans. Smart Grid*, vol. 3053, no. c, pp. 1–11, 2018.
- [21] N. Rezaei and M. Kalantar, "Stochastic frequency-security constrained energy and reserve management of an inverter interfaced islanded microgrid considering demand response programs," *Int. J. Electr. Power Energy Syst.*, vol. 69, pp. 273–286, 2015.
- [22] S. Zhang, J. Yang, X. Wu, and R. Zhu, "Dynamic power provisioning for cost minimization in islanding micro-grid with renewable energy," *2014 IEEE PES Innov. Smart Grid Technol. Conf. ISGT 2014*, pp. 0–4, 2014.
- [23] D. E. Olivares, C. A. Canizares, and M. Kazerani, "A centralized energy management system for isolated microgrids," *IEEE Trans. Smart Grid*, vol. 5, no. 4, pp. 1864–1875, 2014.
- [24] Y. Li, T. Zhao, P. Wang, H. B. Gooi, L. Wu, Y. Liu, and J. Ye, "Optimal operation of multimicrogrids via cooperative energy and reserve scheduling," *IEEE Trans. Ind. Informatics*, vol. 14, no. 8, pp. 3459–3468, 2018.
- [25] IEEE Std 1547.4, *IEEE Guide for Design, Operation, and Integration of Distributed Resource Island Systems with Electric Power Systems IEEE Standards Coordinating Committee 21 Sponsored by the*, no. July. 2011.
- [26] Q. Wang, Y. Guan, and J. Wang, "A chance-constrained two-stage stochastic program for unit commitment with uncertain wind power output," *IEEE Trans. Power Syst.*, vol. 27, no. 1, pp. 206–215, 2012.
- [27] Y. G. Rebours, D. S. Kirschen, M. Trotignon, and S. Rossignol, "A survey of frequency and voltage control ancillary services - Part I: Technical features," *IEEE Trans. Power Syst.*, vol. 22, no. 1, pp. 350–357, 2007.
- [28] J. T. Saraiva and M. H. Gomes, "Provision of some ancillary services by microgrid agents," *2010 7th Int. Conf. Eur. Energy Mark. EEM 2010*, pp. 1–8, 2010.
- [29] I. Gorooi Sardou, M. E. Khodayar, K. Khaledian, M. Soleimani-Damaneh, and M. T. Ameli, "Energy and Reserve Market Clearing with Microgrid Aggregators," *IEEE Trans. Smart Grid*, vol. 7, no. 6, pp. 2703–2712, 2016.
- [30] A. Majzoobi and A. Khodaei, "Application of microgrids in providing ancillary services to the utility grid," *Energy*, vol. 123, pp. 555–563, 2017.
- [31] C. A. Baone, N. Acharya, and H. L. N. Wiegman, "Optimal day-ahead scheduling for microgrid participation in frequency regulation markets," *2016 IEEE Power Energy Soc. Innov. Smart Grid Technol. Conf. ISGT 2016*, pp. 1–5, 2016.
- [32] C. Yuen, A. Oudalov, and A. Timbus, "The provision of frequency control reserves from multiple microgrids," *IEEE Trans. Ind. Electron.*, vol. 58, no. 1, pp. 173–183, 2011.
- [33] S. Qin, "Quantification of Ancillary Service Provision by Microgrid," *Core.ac.uk*, 2019. [Online]. Available: <https://core.ac.uk/display/41901537>.
- [34] J. Wang, H. Zhong, Q. Xia, Z. Ma, Z. Wang, and X. Wu, "Robust Bidding Strategy for Microgrids in Joint Energy, Reserve and Regulation Markets," *2017 IEEE Power & Energy Society General Meeting*, Chicago, IL, 2017, pp. 1–5.
- [35] G. Liu, S. Member, Y. Xu, and K. Tomsovic, "Bidding Strategy for Microgrid in Day-Ahead Market Based on Hybrid Stochastic / Robust," *IEEE Trans. on Smart Grid*, vol. 7, no. 1, pp. 227–237, Jan. 2016.
- [36] D. T. Nguyen and L. B. Le, "Optimal bidding strategy for microgrids considering renewable energy and building thermal dynamics," *IEEE Trans. Smart Grid*, vol. 5, no. 4, pp. 1608–1620, 2014.
- [37] J. Wang, H. Zhong, W. Tang, R. Rajagopal, Q. Xia, C. Kang, and Y. Wang, "Optimal bidding strategy for microgrids in joint energy and ancillary service markets considering flexible ramping products q," *Appl. Energy*, vol. 205, pp. 294–303, 2017.
- [38] P. Dash, "Power exchange for frequency control (PXFC)," *IEEE PES Winter Meet. 1999*, pp. 809–819 vol.2, 1999.
- [39] G. J. Lim, M. Rungta, M. R. Baharnemati, "Reliability analysis of evacuation routes under capacity uncertainty of road links Reliability analysis of evacuation routes under capacity uncertainty of road links," *IIEE Transactions* 0:0, pages 1-15.
- [40] T. Li and M. Shahidehpour, "Price-based unit commitment: a case of Lagrangian relaxation versus mixed integer programming," *IEEE Trans. Power Syst.*, vol. 20, no. 4, pp. 2015–2025, 2005.
- [41] Z. Wu, P. Zeng, X. P. Zhang, and Q. Zhou, "A Solution to the Chance-Constrained Two-Stage Stochastic Program for Unit Commitment with Wind Energy Integration," *IEEE Trans. Power Syst.*, vol. 31, no. 6, pp. 4185–4196, 2016.
- [42] IBM CPLEX, Available at: <https://www.ibm.com/analytics/cplex-optimizer>. [accessed 2019].

Yiwei Wu is currently a Ph.D. student in the Industrial Engineering Department at the University of Houston, USA. His research interests include mathematical modeling, microgrid, power system market, robust optimization, and smart grid.

Gino J. Lim is Chairman and Professor of Industrial Engineering, and Hari and Anjali Faculty Fellow at the University of Houston. He is a fellow of IIEE, and holds a Ph.D. in Industrial Engineering from University of Wisconsin-Madison. His research interest lies in developing optimization techniques for solving large scale decision making problems in such areas as network resiliency, homeland security, power systems, healthcare, and transportation networks. His e-mail address is ginolim@uh.edu.

Jian Shi received his Ph.D. degree in electrical and computer engineering from Mississippi State University in 2014. Presently, he is an assistant professor in the Engineering Technology Department at the University of Houston. His research interest lies in microgrid modeling and control, transportation electrification, and cyber-physical power systems.